Mem. Fac. Agr. Kagoshima Univ., **16**, 129–156, 1980

Creep Deformation of Cohesive Soils and its Relationship to Landslide

Etsuro SHIMOKAWA
(*Laboratory of Erosion Control*)
Received for Publication September 3, 1979

Introduction

Both deformation and strength behaviors of cohesive soils such as landslide clay have time dependent properties. Creep, namely the progress of deformation with lapse of time under a constant sustained load is a time dependent phenomenon of cohesive soils. There are not a few creep type landslides among them. Both the landslide displacement and slope stability of this type may be related to the creep deformation and creep strength of the clay. Consequently, it is considered that the occurrence of landslides can be predicted by the application of these relationships.

In order to predict landslides, fundamental studies must be carried out about the creep deformation of cohesive soils.

According to the previous study[20], the creep deformation characteristics under an upper yield value differ from those over the upper yield value for cohesive soil. The creep deformation stops in time under the upper yield value. Contrary to this, cohesive soil causes creep failure over the upper yield value. Creep deformation is commonly expressed by the strain-time relation (creep curve). The previous studies[7, 20, 32, 33] were performed in order to express numerically the relationship. The greater part of the studies is related to the creep deformation under the upper yield value. But, the creep deformation of cohesive soils is rich in variety, and there are not a few that do not obey the previous laws, namely logarithmic[20] and exponential laws[32, 33]. In addition, in the previous studies the changes of effective stress during the creep were not considered. Moreover, there are few studies with regard to the stress-strain-time relation for the creep failure of cohesive soils.

This paper is concerned with the creep deformation and creep failure. The purpose of this study is summarized as follows:

1) To grasp the causes of various creep deformations of cohesive soils and their time dependent mechanism.

2) To grasp the mechanism of creep failure and to derive the stress-strain-time relation under the state.

3) To analyze the displacement of landslide and slope stability according to the creep deformation of cohesive soils. The experimental and theoretical studies were carried out for those purposes. Part 1, part 2 and part 3 of this paper are accompanied with some corrections of the two previously published papers[30, 31]. The fourth part is a new addition.

Notations

a = coefficient of relationship between the number of bonds per unit area and consolida-

tion pressure

b = coefficient relating reduction of the number of bonds per unit length, s

C = value of logarithmic dilatancy rate in the second creep region

c' = effective cohesion intercept

ΔF = free energy of activation

f = force acting on a bond

h = Planck's constant

k = Boltzmann's constant

k = coefficient of relationship between logarithmic dilatancy rate and effective stress ratio

m = coefficient relating reduction of the number of bonds per unit length, s

N, N_0 = number of bonds per unit area and its initial number, respectively

s = number of bonds per unit length

R = gas constant

T = absolute temperature

t = time

t_b = a standard time

t_f = elapsed time to failure

u = excess pore water pressure

v = volumetric strain

$\frac{dv}{d\log_{10} t}$ = logarithmic volumetric strain rate

α, β = coefficient relating creep stress dependency of logarithmic strain rate

γ = shear strain

γ_b = shear strain at a standard time t_b

$\frac{d\gamma}{d\log_{10} t}$ = logarithmic shear strain rate

ε = strain

ε_1, ε_3 = maximum principal strain and minimum principal strain, respectively

ε_f = strain at failure

$\frac{d\varepsilon}{dt}$ = strain rate

$\frac{d\varepsilon}{d\log t}$ = logarithmic strain rate

$\left(\frac{d\varepsilon}{d\log t}\right)_f$ = logarithmic strain rate at failure

$\eta_{app.}$ = apparent coefficient of viscosity

λ, λ' = a mean distance between bonds

$\bar{\nu}$ = frequency of activation

σ_1', σ_3' = maximum principal effective stress and minimum principal effective stress, respectively

σ_c = consolidation pressure

σ_d = deviator stress

σ_{df} = deviator stress at failure

σ_{dD} = dilatancy component of strength

σ_{dF} = friction component of strength

σ_{dV} = viscosity component of strength

σ_d/σ_{df} = creep stress level

σ_m' = mean principal effective stress

σ_{m0}' = mean effective consolidation pressure

σ_d/σ'_m = effective stress ratio
σ_N = normal stress
τ = shear stress
τ_f = shear stress at failure
τ/τ_f = creep stress level
ϕ' = angle of shearing resistance

Methods

Materials investigated in this test programme are Kirishima, Yame and Hirayama landslide clays, Tatara clay (Tertiary), Hayato clay (Quaternary) and Toyoura sand. Their physical properties are shown in Table 1. The specific gravity of 2.457 for Hayato clay is unusually small, because this clay is originated in the second deposit of the pyroclastic flow. The plasticity index is in a wide range from the Hayato clay of 13.3 to the Kirishima clay of 67.6. Toyoura sand is non-plastic.

Table 1. Physical properties of soils

	Specific gravity of grains	Liquid limit, %	Plastic limit, %	Plasticity index	Clay fration, %
Yame clay	2.749	40.0	16.9	23.1	22.2
Kirishima clay	2.562	108.5	40.9	67.6	—
Hirayama clay	2.59	89.8	42.4	47.4	44.8
Tatara clay	2.645	76.9	50.4	26.5	25.6
Hayato clay	2.457	40.7	27.4	13.3	40.0
Toyoura sand	2.67				

Normally consolidated specimens of the disturbed clays were remolded in a state of water content over the liquid limit of these clays and were consolidated under a consolidation pressure of 1 and 0.4 kg/cm^2 in a consolidation container. Over-consolidated specimens of the disturbed clay were consolidated one-dimensionally under the consolidation pressure of 10 kg/cm^2 in a cylindrical tube having a diameter of 3.4 cm and 10.5 cm in height and were unloaded after that. Hirayama undisturbed specimens were formed into a cylindrical shape so that the sliding surface in the direct shear tests agrees with that at the landslide field, which were obtained from the sliding surface of Hirayama landslide at a depth of about 60 m. The specimens used for the triaxial compression tests and direct shear tests have a diameter of 3.4, 6.0 cm and are 8.0, 2.0 cm in height, respectively. Toyoura sand specimens with a diameter of 5.0 cm and 12.5 cm in height were prepared by pouring the material of 0.5 per cent in water content into a mold. All the specimens were in a saturated state. Physical properties of these specimens are shown in Table 2.

LS typed triaxial compression test and Karol typed direct shear test equipments were used for the experiments. The experiments consist of four methods. The test conditions are summarized in Table 3.

1. Undrained triaxial compression creep test

In order to reduce friction, the upper and lower ends of the specimens were encased by two plastic plates with grease. The specimen was consolidated isotropically under the consolidation

Table 2. Physical properties of samples

Specimen	Specimen condition	Water content, %	Void ratio
Triaxial shear test			
Kirishima clay	Remolded	78.1	1.941
Yame clay	Remolded	24.2	0.664
Hirayama clay	Remolded	59.0	1.571
Tatara clay	Remolded	54.4	1.459
Hayato clay	Remolded	37.0	0.926
Toyoura sand	—	26.7	0.696
Direct shear test			
Kirishima clay	Remolded	93.7	2.518
Hirayama clay	Undisturbed	31.8	0.876

Table 3. Test conditions

Test apparatus	Specimen	Specimen condition	Drained condition	Consolidation condition	Consolidation pressure, kg/cm²	Loading method
Triaxial	Yame clay	Remolded Virgin	Undrained	Normally consolidated	1.0, 2.0	Creep
	Kirishima clay			Normally consolidated Over-consolidated (OCR 10)	1.0, 2.0 1.0	
	Hirayama clay			Normally consolidated	1.0, 2.0	
	Toyoura sand	—		—	0.5	
Triaxial	Yame clay	Remolded Virgin	Undrained	Normally consolidated	1.0, 2.0	Strain controlled
	Kirishima clay				1.0, 2.0	
	Hirayama clay				1.0, 2.0 3.0, 8.0	
Triaxial	Yame clay	Remolded Virgin Preloaded	Drained	Over-consolidated (OCR 2)	2.0→1.0	Creep
	Tatara clay				2.0→1.0	
	Hayato clay				2.0→1.0	
Direct	Kirishima clay	Remolded Preloaded	Drained	Over-consolidated (OCR 2)	0.4→0.2	Creep
	Hirayama clay	Undisturbed Residual			5.0	

pressure of σ_c for 1.5 days and was held up by applying a back pressure of 1.0 kg/cm² for 0.5 days in this test. The value of the back pressure and the length of application time for Toyoura sand was 0.5 kg/cm² and two or three hours, respectively. Creep stress σ_d was applied momentarily, and then was controlled according to the deformation of the specimen. The axial strain was measured by a dial gauge. Excess pore water pressure was measured at the bottom of the specimen through a paper drain encasing it. This test was carried out at a temperature from 25°C to 30°C.

2. Undrained strain-controlled triaxial compression test

There are five loading speeds in this experiment, namely 0.0014, 0.011, 0.016, 0.032 and 0.096 per cent per 1 minute. The others were carried out in the same manner as in the undrained triaxial compression creep test.

3. Drained triaxial compression creep test

This experiment was carried out in virgin and preloaded specimens (specimens which had failed in the creep deformation previously). These specimens were consolidated isotropically under the consolidation pressure of 2.0 kg/cm^2 for 1.5 days, and then were expanded under the consolidation pressure of 1.0 kg/cm^2 for 2.0 days. The volume change was measured by a burette connected with the bottom of the specimen. The temperature in this experiment was within the range from 20°C to 25°C. The others were carried out in the same manner as in the undrained triaxial compression creep test.

4. Direct shear creep test

This experiment was conducted by making use of preloaded Kirishima clay (ruptured under a constant sustained load beforehand) and of the residual undisturbed Hirayama clay. The former specimens were consolidated one-dimensionally under the consolidation pressure of 0.4 kg/cm^2 for 0.5 days, and then were expanded under that of 0.2 kg/cm^2 for 0.5 days in the shear box. The horizontal and normal displacements were measured by two dial gauges. The temperature in this experiment was within the range from 20°C to 25°C.

Part 1. Creep deformations of cohesive soils

Results

1. Undrained triaxial compression creep test

Fig. 1 shows axial strain ε_1-logarithmic time $log_{10} t$ and excess pore water pressure u-logarithmic time relationships for the normally consolidated Kirishima clay. The numbers in this

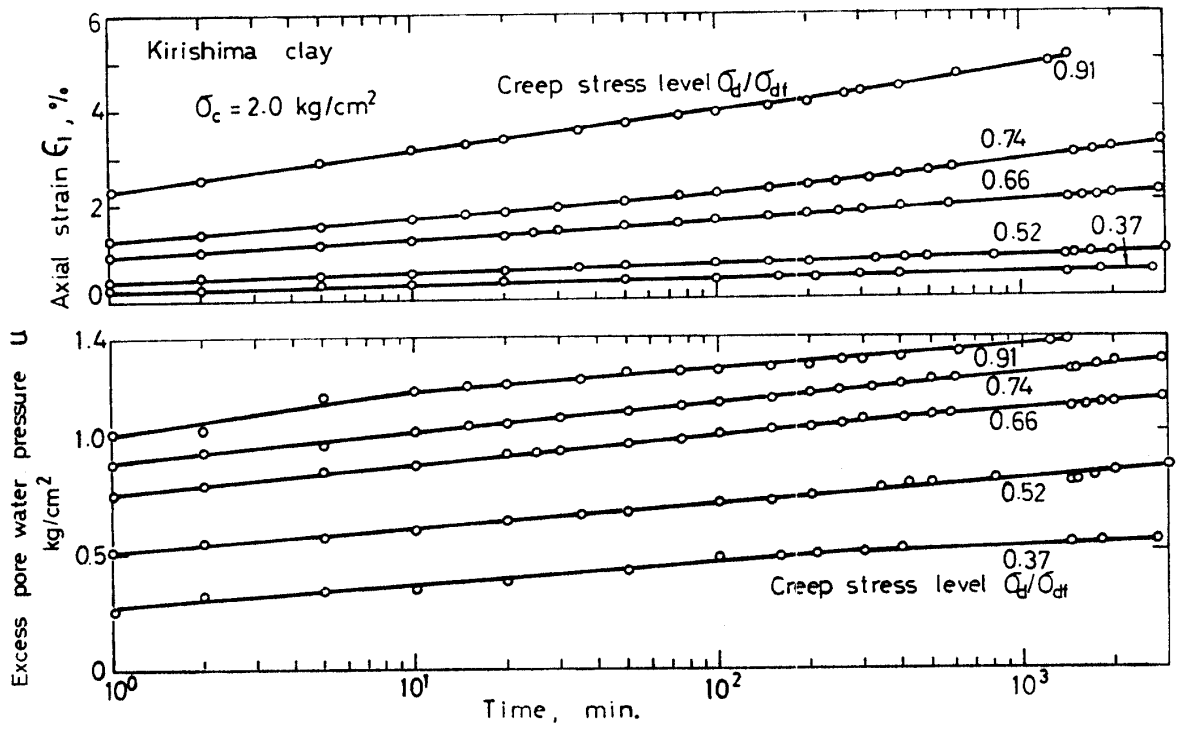

Fig. 1. Axial strain, excess pore water pressure versus logarithmic time for normally consolidated Kirishima clay.

figure express the creep stress level σ_d/σ_{df}, in which σ_d is the creep stress, and σ_{df} the creep stress for the elapsed time to creep failure of 1 minute. Depending on this figure, the axial strain is linear versus logarithmic time and the degree of its change, namely logarithmic strain rate increases with the creep stress level. The excess pore water pressure-logarithmic time relationship is roughly linear, but the degree of its change, namely logarithmic excess pore water pressure rate is constant without creep stress.

The axial strain and excess pore water pressure versus logarithmic time are shown for the normally consolidated Hirayama clay in Fig. 2. The creep deformation characteristic of Hirayama clay is different from that of Kirishima clay. The axial strain-logarithmic time relationship is linear under the low creep stress levels, but shows a singmoid curve under the high creep stress levels. In this case, the inflection points of the curves lie in from 100 to 200 minutes. The logarithmic strain rate under the high creep stress levels is roughly constant after 400 minutes. The excess pore water pressure-logarithmic time relationship is like that between the axial strain and logarithmic time, but the logarithmic excess pore water pressure rate is constant without the creep stress level.

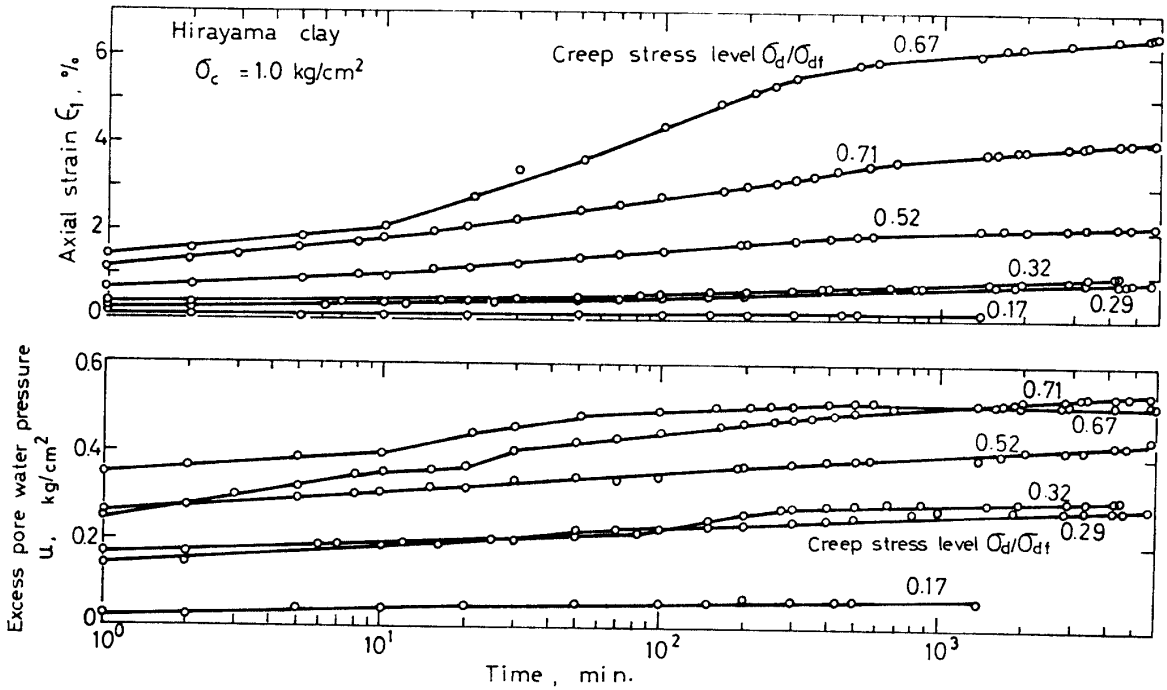

Fig. 2. Axial strain, excess pore water pressure versus logarithmic time for normally consolidated Hirayama clay.

Fig. 3 shows the axial strain and excess pore water pressure-logarithmic time relationships for the normally consolidated Yame clay. The axial strain-logarithmic time relationship is like that of Hirayama clay except the inflection point of the singmoid curve lying in 40 minutes.

The greater part of the axial strain and excess pore water pressure occurred momentarily for the creep test of Toyoura sand. Therefore, creep strain did not occur. The excess pore water pressure is all negative.

2. Drained triaxial compression creep test

The axial strain and volumetric strain-logarithmic time relationships are shown for the over

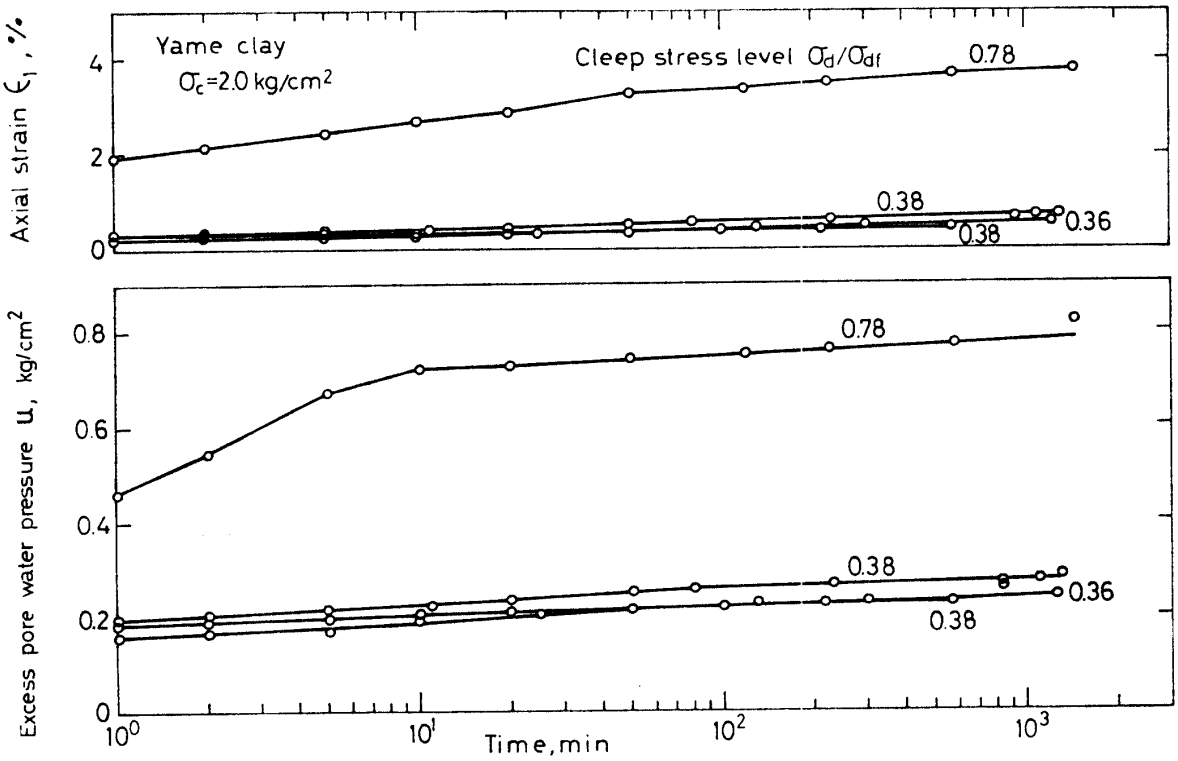

Fig. 3. Axial strain, excess pore water pressure versus logarithmic time for normally consolidated Yame clay.

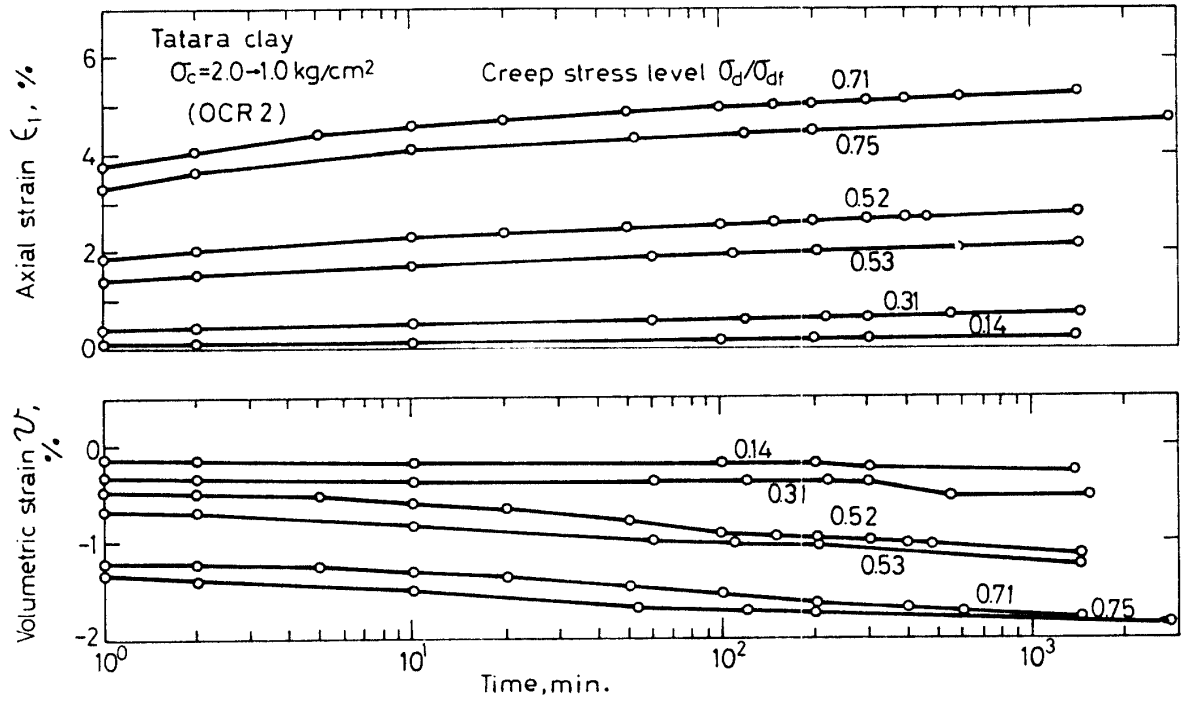

Fig. 4. Axial strain, volumetric strain versus logarithmic time for over-consolidated Tatara clay.

consolidated Tatara clay in Fig. 4. The relationship between the axial strain and logarithmic time is linear under the low creep stress levels, but is unlinear under the high creep stress levels. The volumetric strain-logarithmic time relationship is like that between the axial strain and logarithmic time.

Fig. 5 shows the axial strain and volumetric strain versus logarithmic time in the preloaded state for Hayato clay. In this state, the axial strain-logarithmic time relationship is linear without the creep stress. And, the values of the axial strain and logarithmic strain rate are smaller compared with those of the virgin. The volumetric strain can be neglected.

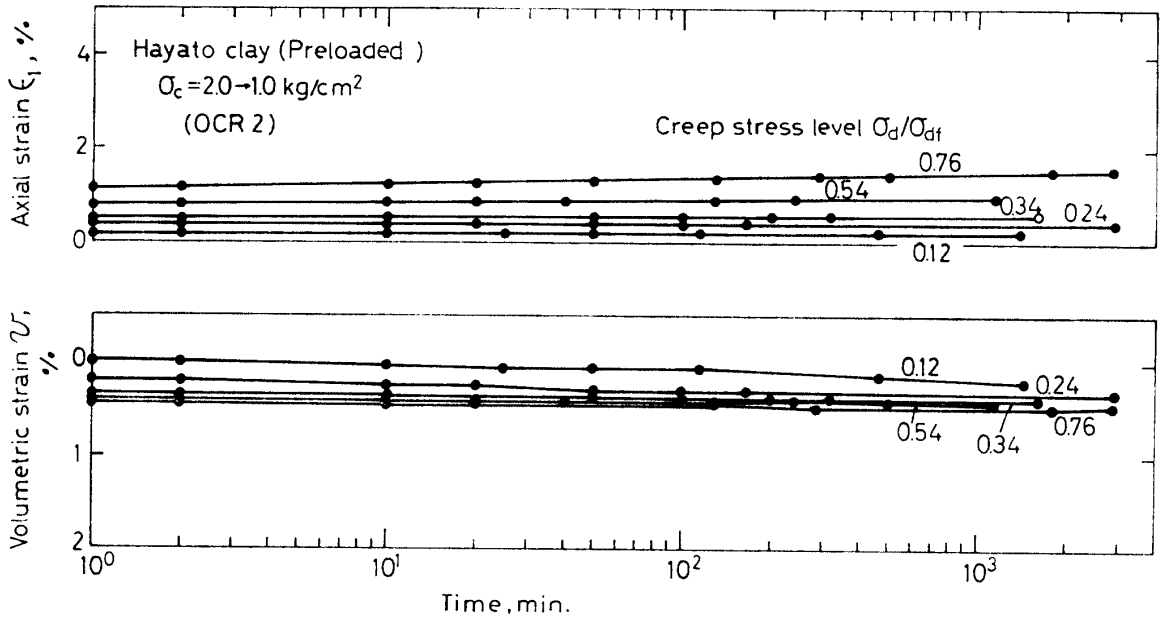

Fig. 5. Axial strain, volumetric strain versus logarithmic time in the preloaded state of Hayato clay.

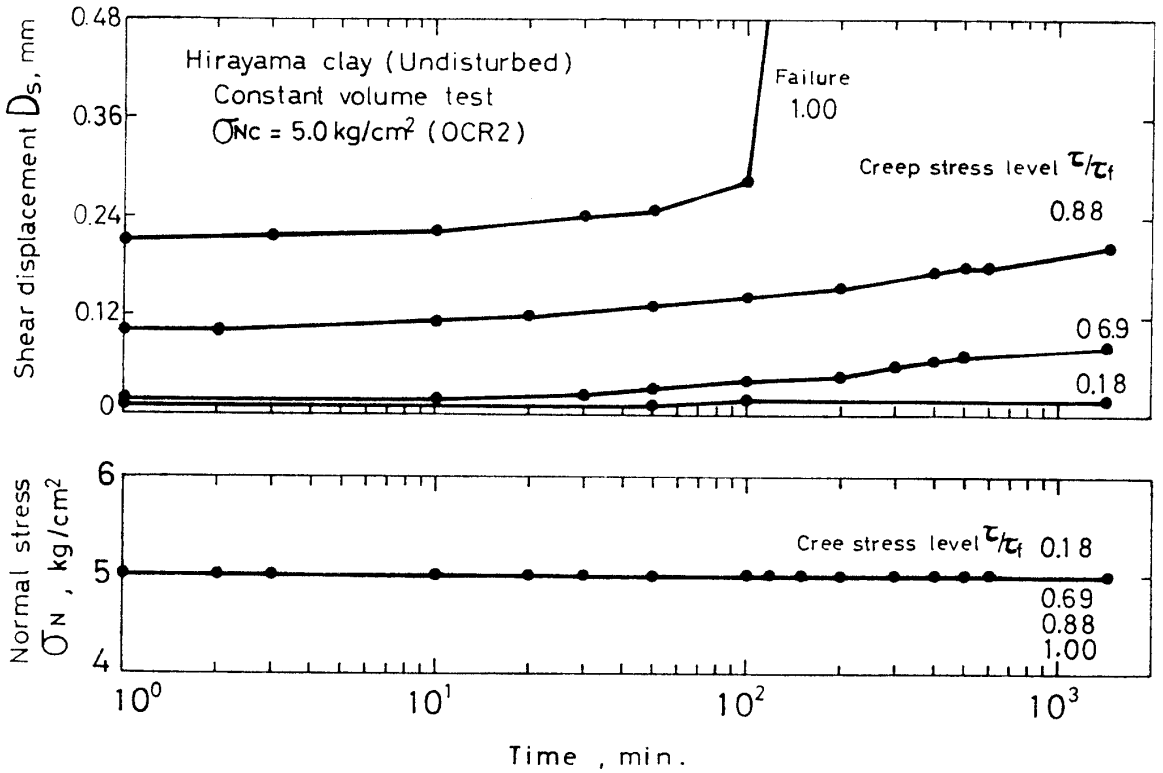

Fig. 6. Shear displacement, normal stress versus logarithmic time in the residual state of undisturbed Hirayama clay.

3. Direct shear creep test

Fig. 6 shows horizontal displacement D_s and normal stress σ_N-logarithmic time relationships for the volume constant test of the undisturbed Hirayama clay in the residual state. In this figure, the numbers of the curves show the creep stress level τ/τ_f, in which τ is the creep stress and τ_f the creep failure stress. According to this figure, the horizontal displacement versus logarithmic time is linear, or shows a slightly concave curvature in the upper part. The normal stress is not changed.

Discussion

The creep deformations of cohesive soils are to be grouped into the following four types according to the pattern of the strain-logarithmic time, namely creep curve.

① The creep strain versus logarithmic time is linear without the creep stress level and the logarithmic creep strain rate is large in degree.

② The creep strain versus logarithmic time is linear under the low creep stress levels, but shows a pattern such as a singmoid curve under the high creep stress levels.

③ The greater part of the strain occurs momentarily.

④ The creep strain is linear without the creep stress level versus logarithmic time, and the logarithmic strain rate is small in degree. Dilatancy is small in value, or does not occur. This type is that of the creep deformation for the preloaded and residual states.

In order to explain the mechanism of the four types, an analysis with regard to components of the creep deformation have to be done. Three fundamental components will be assumed as shown in Fig. 7. Elasticity is composed of the time independent and time dependent elasticity. The

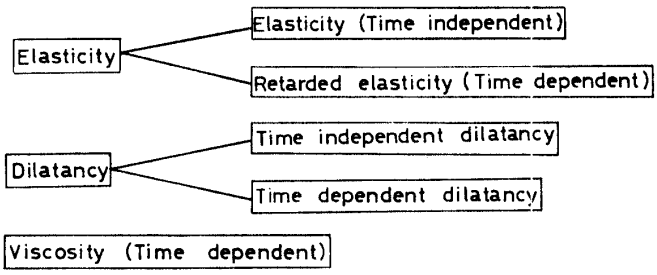

Fig. 7. Components of creep deformation.

elastic strain and retarded elastic strain are due to the time independent elasticity and time dependent elasticity, respectively. The elasticity is based on the elastic geometrical changes of the soil skeleton. Dilatancy is composed of the time independent dilatancy and time dependent dilatancy. This originates in viscoplastic changes of the soil skeleton. Viscosity is based on the absorbed water film around the soil particles. This component has a time dependent property, and influences the creep strain due to the sliding between the soil particles, retarded elasticity and time dependent dilatancy. The components are mobilized in the order of elasticity and time independent dilatancy firstly, and retarded elasticity, time dependent dilatancy and viscosity, secondly. The creep deformation for a long period is caused by the retarded elasticity, time dependent dilatancy and viscosity. The properties and degree of mobilization of the components differ with the soil properties and stress states.

Now, consider the creep deformation in the triaxial compression state. Denoted by ε_1, ε_3 the principal strain, v the volumentric strain and γ the shear strain, v is expressed by the next

equation

$$v=\varepsilon_1+2\varepsilon_3 \tag{1}$$

γ is expressed by the next equation

$$\gamma=\frac{2}{3}(\varepsilon_1-\varepsilon_3) \tag{2}$$

By substituting Eq. (1) into Eq. (2)

$$\varepsilon_1=\frac{1}{3}v+\gamma \tag{3}$$

By differentiating Eq. (3) with respect to $log_{10}\,t$

$$\frac{d\varepsilon_1}{d\,log_{10}\,t}=\frac{1}{3}\frac{dv}{d\,log_{10}\,t}+\frac{d\gamma}{d\,log_{10}\,t} \tag{4}$$

can be obtained. According to Eq. (4), the first term in the right hand expresses the logarithmic dilatancy rate. This term influences both the logarithmic shear strain rate and logarithmic axial strain rate. In the undrained triaxial compression creep tests, this is equivalent to the logarithmic excess pore water pressure rate. Fig. 8 and Fig. 9 show the relationship between the logarithmic excess pore water pressure rate and creep stress for the creep test of Hirayama clay and Kirishima clay, respectively. The logarithmic excess pore water pressure rate increases in value with time, and shows the maximum value at about 100 minutes. After that, it decreases with the lapse of

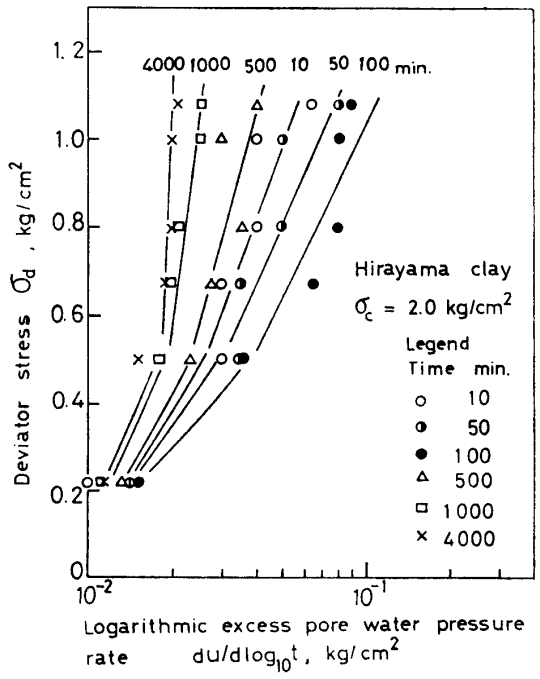

Fig. 8. Relationship between deviator stress and logarithmic excess pore water pressure rate for normally consolidated Hirayama clay.

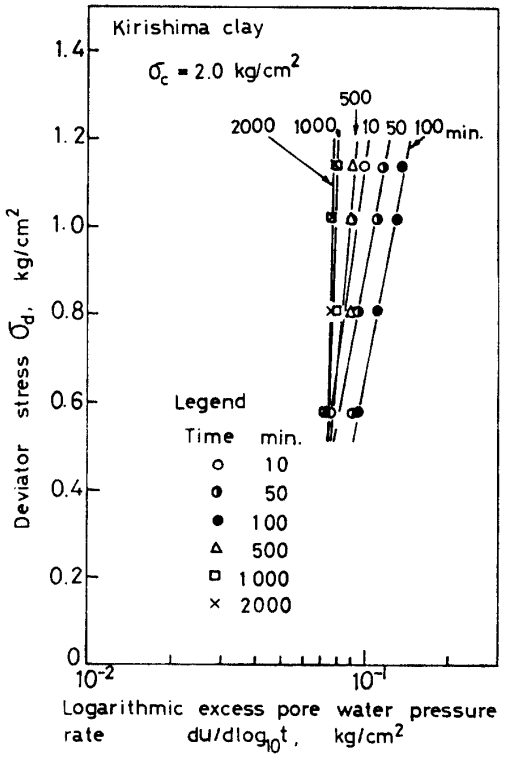

Fig. 9. Relationship between deviator stress and logarithmic excess pore water pressure rate for normally consolidated Kirishima clay.

time, and is constant without the creep stress after about 1000 minutes. Comparing its creep stress dependency with the creep curve for Hirayama clay, the occurrence time of its maximum and constant values coincide with that of the inflection point and constant logarithmic strain rate region of the creep curve, respectively. This has the same meaning as the logarithmic volumetric strain rate (logarithmic dilatancy rate) is constant without effective creep stress as pointed out by Walker[38]. Moreover, the logarithmic excess pore water pressure rate and its creep stress dependency characteristics for Hirayama clay differ from those of Kirishima clay. Difference of the creep curve for the two clays under the high creep stress levels may be caused by the above mentioned reason.

Dividing into the first and second creep regions by the creep stress dependency of the logarithmic dilatancy rate

$$\frac{dv}{d\log_{10} t} = k \frac{\sigma_d}{\sigma'_m} \tag{5}$$

$$\frac{dv}{d\log_{10} t} = Const. = C \tag{6}$$

can be obtained, in which σ_d is the deviator stress, σ'_m the effective mean principal stress and C, k the constants. The logarithmic dilatancy rate by Eq. (5) is time independent. Contrary to Eq. (5), the logarithmic dilatancy rate expressed by Eq. (6) is time dependent. Substituting Eq. (5) and Eq. (6) into Eq. (4), respectively

$$\frac{d\varepsilon_1}{d\log_{10} t} = \frac{1}{3} k \frac{\sigma_d}{\sigma'_m} + \frac{d\gamma}{d\log_{10} t} \tag{7}$$

$$\frac{d\varepsilon_1}{d\log_{10} t} = \frac{1}{3} C + \frac{d\gamma}{d\log_{10} t} \tag{8}$$

According to Eq. (7), the time independent dilatancy in the first creep region is as large as the creep stress level. The time dependent dilatancy in the second creep region is constant by Eq. (8). Therefore, the deformation in the second creep region is influenced by the retarded elasticity, time dependent dilatancy and viscosity. Fig. 10 shows the schematic representation of the components of the creep deformation versus logarithmic time.

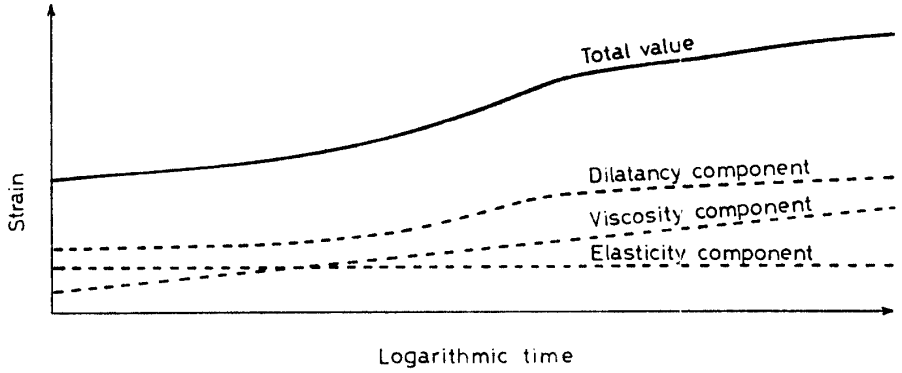

Fig. 10. Schematic representation relating the components of creep deformation versus logarithmic time.

In the preloaded and residual states, there is no effect by the time dependent dilatancy on the creep deformation of cohesive soils. Hence, the first term in the right hand of Eq. (4)

$$\frac{1}{3}\frac{dv}{d\log_{10} t} \fallingdotseq 0 \tag{9}$$

Eq. (4)

$$\frac{d\varepsilon_1}{d\log_{10} t} = \frac{d\gamma}{d\log_{10} t} \tag{10}$$

The creep strain is linear versus logarithmic time in these states.

Next, consider a relationship between the logarithmic creep strain rate in the second creep region and creep stress. This relationship is shown in Fig. 11 for the undrained triaxial compression creep test of the three normally consolidated clays and in Fig. 12 for the drained triaxial compres-

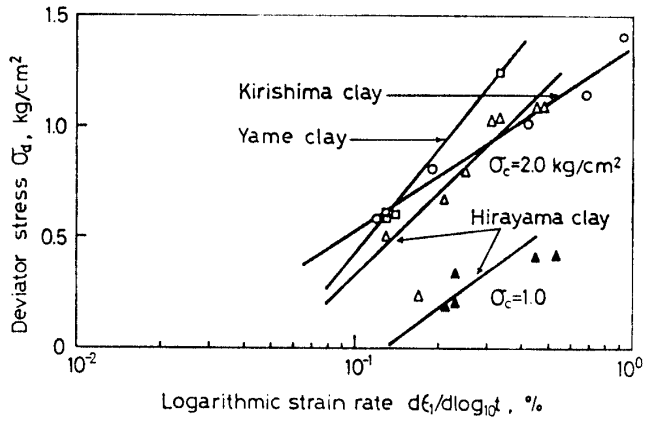

Fig. 11. Relationship between deviator stress and logarithmic strain rate for normally consolidated clays.

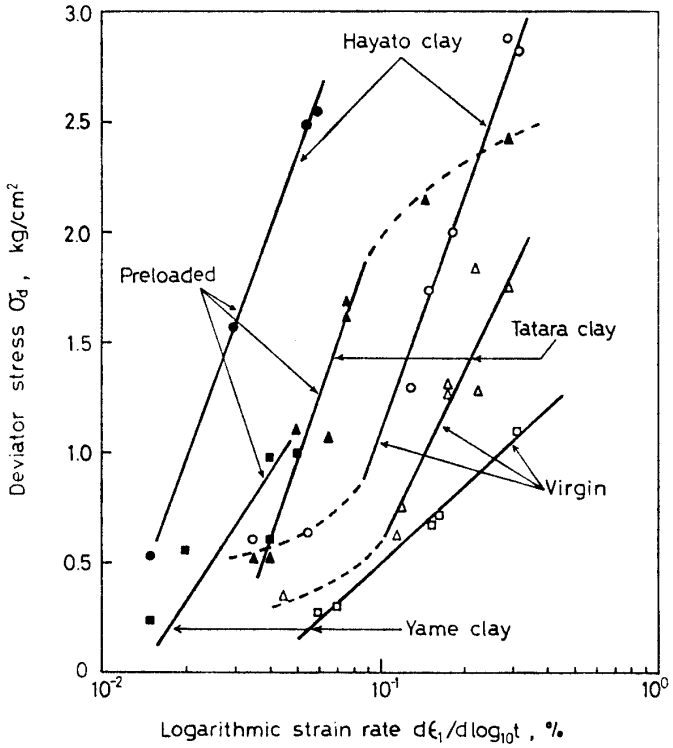

Fig. 12. Relationship between deviator stress and logarithmic strain rate for over-consolidated clays.

sion creep test in the virgin and preloaded states of three lightly over-consolidated clays. According to the figures, this relationship is linear on semilog co-ordinates. Hence,

$$log_{10}\frac{d\varepsilon_1}{d\,log_{10}t}=\alpha+\beta\sigma_d \tag{11}$$

is obtained, where α and β are the constants. An angle β of the straight line is a parameter showing the stress dependency of the second creep deformation. The value of the parameter β becomes smaller in the following order, Kirishima clay, Hirayama clay and Yame clay. And, the value in the preloaded state is smaller than that in the virgin state. In other words, the parameter β may depend on the soil properties and stress states, etc.. This difference may be based on the components of the creep deformation, namely the retarded elasticity, time dependent dilatancy and viscosity. A sliding surface is formed for the cohesive soil under a high creep stress level, along which the clay particles are re-oriented.

The reduction of parameter β due to the stress history will be based on the changes of the clay skeleton. Fig. 13 shows the relationship between the reciprocal of parameter β and the plasticity index. The reciprocal $\frac{1}{\beta}$ is expressed by the ratio of the creep stress to the logarithmic axial strain rate, which is like the coefficient of viscosity. The reciprocal $\frac{1}{\beta}$ reduces with the plasticity index of cohesive soils, and it depends on the stress history.

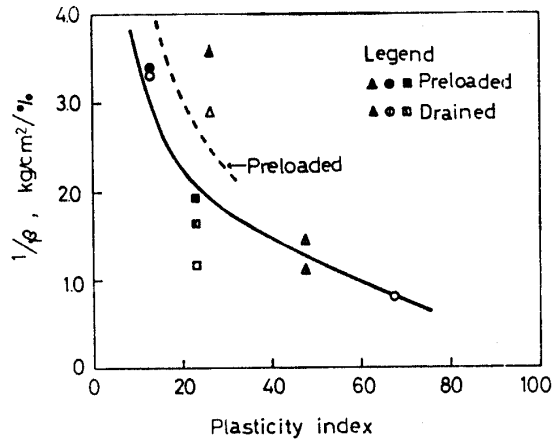

Fig. 13. Relationship between $1/\beta$ and plasticity index.

Part 2. Creep failure of cohesive soil

Results

1. Normally consolidated clay

Judging from the creep curve of the cohesive soils, the process of creep failure is composed of the first creep (transient creep), second creep (steady state creep) and third creep (accelerated creep). The creep rate decreases gradually in the first creep region and is nearly constant in the second creep region. The minimum creep rate appears in the second creep region. In the third creep region, the creep rate increases gradually, and the specimen fails.

Fig. 14 shows the changes in the effective stress state accompanied by the creep deformation of the normally consolidated Kirishima clay. The stress paths approach a failure line in the left hand by tracing the different courses according to the creep stresses. In this figure, axial equistrain

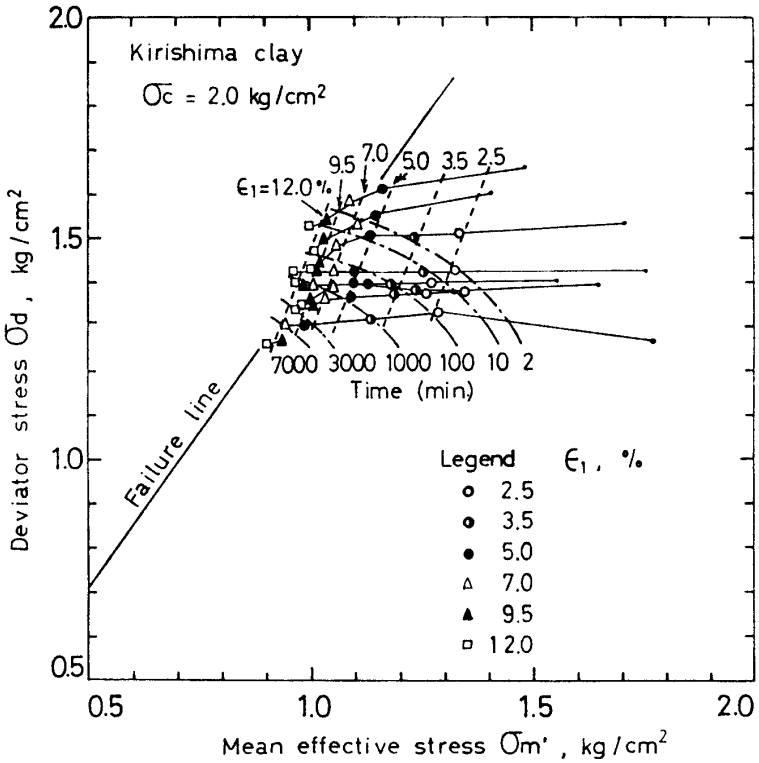

Fig. 14. Stress paths of creep failure for normally consolidated Kirishima clay.

lines and equitime lines are shown. The axial equistrain lines are parallel to a maximum principal axis. This means that the excess pore water pressure is expressed as a function of only the axial strain regardless of the creep stress and creep rate. This result is in agreement with the experimental results of Akai, Adachi and Ando[1] for the constant strain rate test and stress relaxation test, and Murayama, Sekiguchi and Ueda[22] for the stress relaxation test. The relationship between the excess pore water pressure and axial strain is plotted on semilog co-ordinates, Fig. 15.

Fig. 16 shows the relationship between the excess pore water pressure divided by the deviator stress u/σ_d and axial strain. This relationship depends on the creep stress. As stated before, the excess pore water pressure is expressed as the function of only the axial strain.

Fig. 17 shows the time dependency of the creep strength for three normally consolidated clays. The creep strangth decreases linearly versus logarithmic elapsed time to the creep failure.

2. Over-consolidated clay

The relationship between the excess pore water pressure and axial strain, and stress paths for creep failure of the over-consolidated clay differ from those of the normally consolidated clay. Fig. 18 shows the relationship between the excess pore water pressure and axial strain on semilog co-ordinates for over-consolidated Kirishima clay. The excess pore water pressure has a maximum value at an axial strain of about 3.5 per cent, and decreases with axial strain after that. But, it is expressed by the function of only the axial strain in the same manner as in that of the normally consolidated clay. This result differs from the experimental result of Akai, Adachi, Tanaka and Ikeda[2]. Fig. 19 shows the stress paths in the process of creep failure. In the over-consolidated clay, the stress paths pass through the failure line (a maximum effective stress ratio) from the left hand to the right hand. The axial equistrain lines are parallel to the maximum principal stress axis.

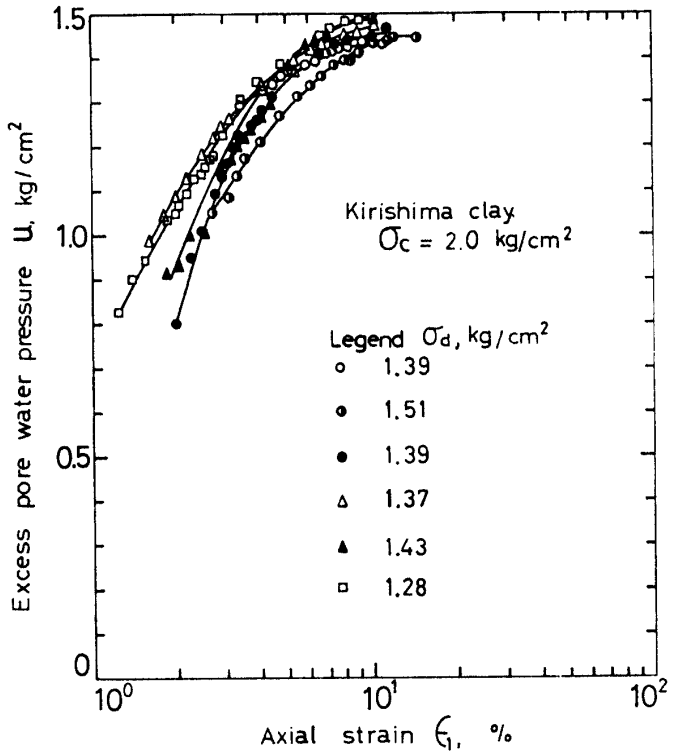

Fig. 15. Relationship between excess pore water pressure and axial strain for normally consolidated Kirishima clay.

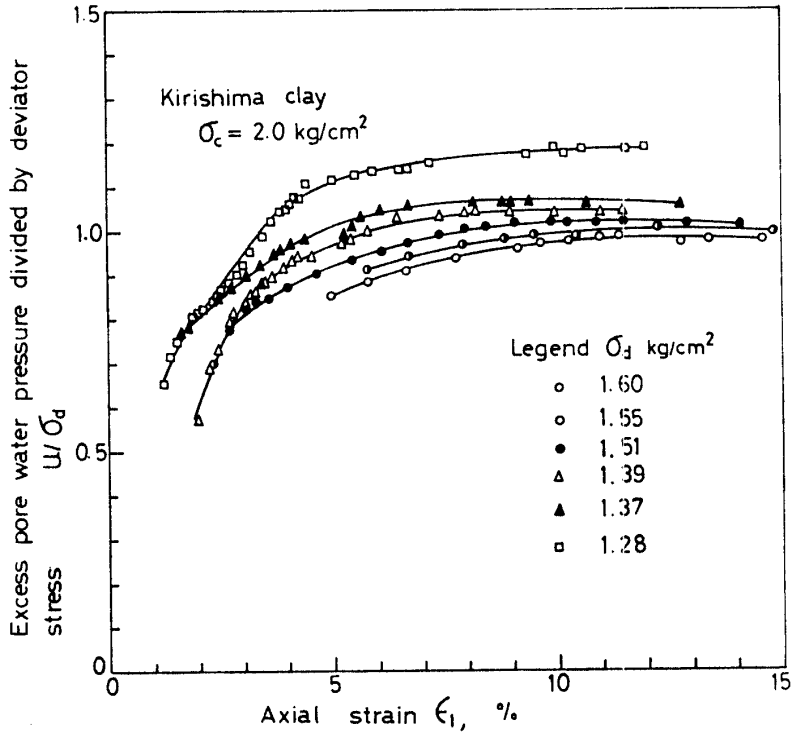

Fig. 16. Relationship between excess pore water pressure divided by deviator stress and axial strain for normally consolidated Kirishima clay.

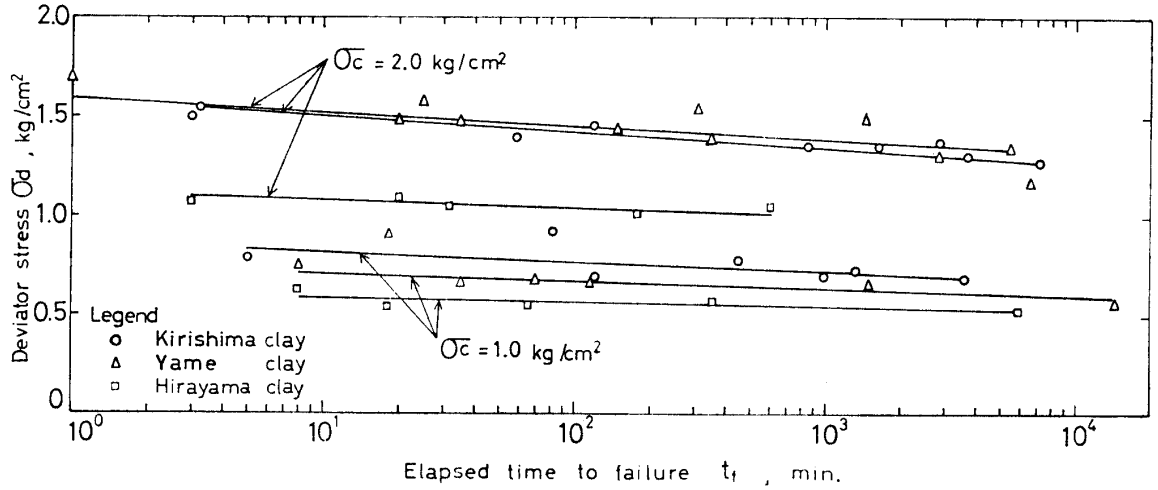

Fig. 17. Influence of elapsed time to creep failure on creep strength of normally consolidated clays.

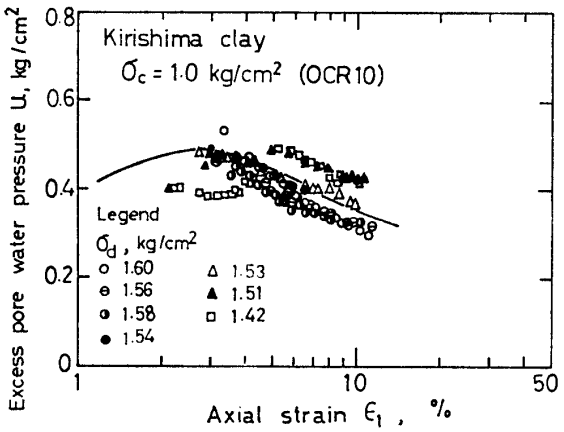

Fig. 18. Relationship between excess pore water pressure and axial strain for over-consolidated Kirishima clay.

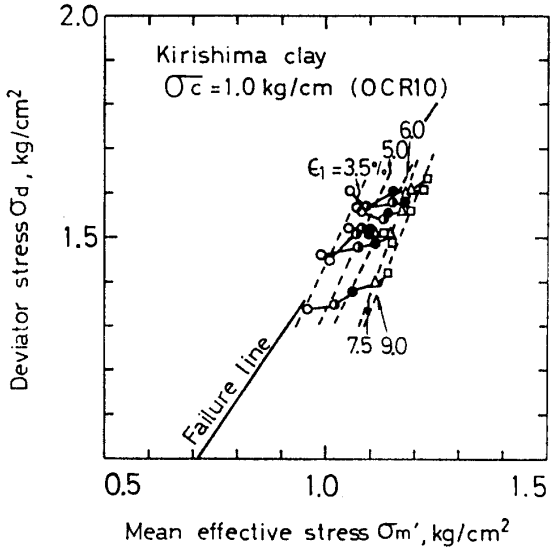

Fig. 19. Stress paths of creep failure for over-consolidated Kirishima clay.

Discussion

1. Deformation characteristics of creep failure

All the external force is not to be applied to the specimen as effective stress simultaneously with the start of creep deformation, but is to be transformed into the effective stress gradually with the progress of creep deformation and time. Therefore, it is assumed that creep failure occurs when all the external force is transformed into the effective stress. In this case, the stress is not in the state of all-round pressure and K_0, but in a state of anisotropic stress.

This manner is shown in Fig. 14 and Fig. 19. The stress paths approach the failure line in the left hand from the right hand, and in the specimen creep failure occurs at the maximum effective stress ratio for the normally consolidated clay. But, the creep failure that is defined by the creep curve occurs under a decrease in the effective stress ratio for the over-consolidated clay. In other words, the effective stress ratio at the creep failure does not show the maximum value. By the way, the axial strain at maximum effective stress ratio is about 3.5 per cent, which belongs to the first

creep region. The axial strain at creep failure is about 7.0 per cent, which agrees with that at the maximum deviator stress for the constant strain rate test. The effective stress ratio corresponds to the imaginary internal friction angle.

Some peculiar changes appear in the process of creep failure. Fig. 20 shows the stress states at the beginning of the second and third creep regions and creep failure for the normally consoli-

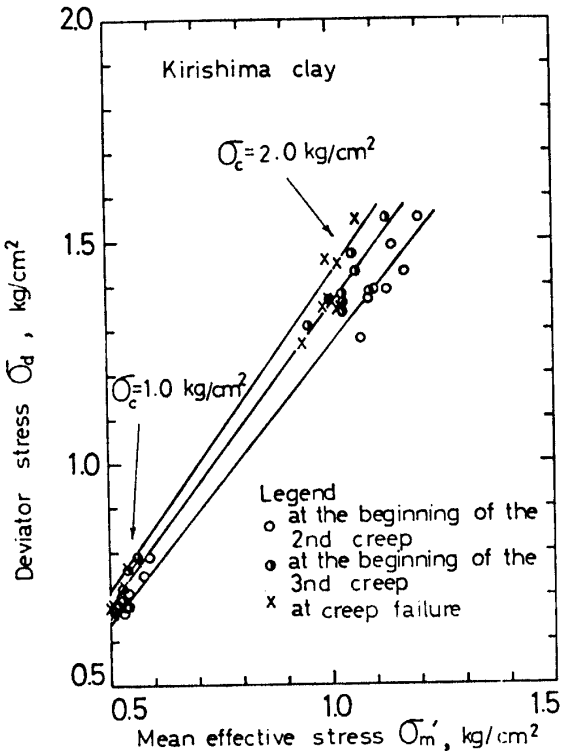

Fig. 20. Effective stresses at the beginning of the second and third creep and creep failure for normally consolidated Kirishima clay.

dated clay. The effective stress states at these critical strains are plotted on the three straight lines drawn through the origin, respectively. In other words, the effective stress ratios are constant regardless of the creep stresses. The same result is observed also for the over-consolidated clay. This result agrees with that of Murayama, Kurihara and Sekiguchi[21]. This may imply the occurrence of some structural changes connected with the failure from the beginning of the second creep. Vyalov, Pekarskaya and Maximyak[37] pointed out that these changes are composed of the re-orientation of clay particles, and development of micro-fissures and defects.

Fig. 21 shows the critical axial strains at the beginning of the first creep region and second creep region and creep failure for the normally consolidated clays. In this figure, the experimental result of Murayama, Kurihara and Sekiguchi[21] was plotted. The critical axial strains depend on creep stresses. This result contradicts that of Goldstein and Ter-Stepanian[11]. This may be a rheological property of the cohesive soil, that is, the type of deformation differs according to the time scale of observation time in the visco-elastic body.

2. Creep strength

The creep strength depends on the elapsed time to failure as shown in Fig. 17. This property may be caused by the visco-elasticity of the cohesive soil, too. Consider the mechanism of this

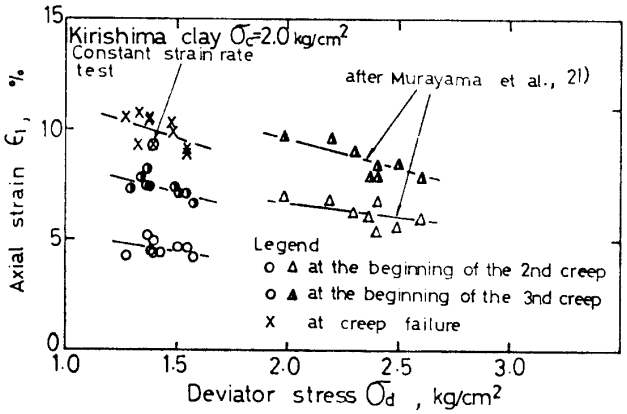

Fig. 21. Influence of deviator stress on axial strains at the beginning of the second and third creep and creep failure for normally consolidated clays.

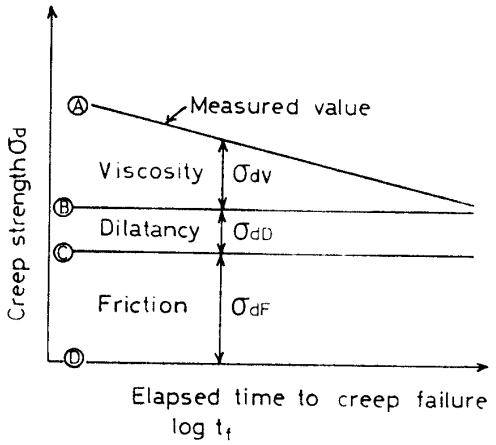

Fig. 22. Schematic representation relating time dependency of creep strength components.

property. Divide the strength of cohesive soils into the three components of friction, dilatancy and viscosity in a manner similar to Lambe[41]. Fig. 22 shows the schematic representation of creep strength and the three strength components versus logarithmic time. In this figure, line Ⓐ represents the measured creep strength, which is time dependent. The friction component is time independent, which is represented by the space σ_{dF} between the line Ⓒ and the line Ⓓ. Hence, the line Ⓒ is parallel to the base line Ⓓ. The dilatancy component is represented by the space σ_{dD} between the line Ⓒ and the line Ⓑ. This component is time independent, because the excess pore water pressure, namely dilatancy is the function of only the axial strain. Therefore, the time dependency of the creep strength is based on only the viscosity component. The viscosity component is represented by the space σ_{dV} between the line Ⓐ and the line Ⓑ. The larger is the elapsed time to creep failure, the smaller is the viscosity component. In order to cause creep failure, the creep stress over total value between the friction component σ_{dF} and dilatancy component σ_{dD} must be applied to the cohesive soil. As the dilatancy component can be neglected in the residual state, the cohesive soil fails under the creep stress over the friction component in this case. Moreover, the time dependency of the creep strength may be influenced by the type of the cohesive soil and its stress states.

The relationship between the time dependency of the creep strength and plasticity index of cohesive soils is shown in Fig. 23. The creep stress ratio divided by logarithmic time expresses the time dependency of the creep strength, quantitatively, in which σ_d is the creep stress and $\sigma_{dt_f=1min.}$ is the creep stress for the elapsed time to creep failure of 1 minute. In this figure, the experimental values and values rearranged from the previous test results of Arulanandan, Shen and Young[3], Bjerrum[5], Casagrande and Wilson[6], Kurihara[16], Linn Finn and Shead[17], Murayama and Shibata[20], Murayama, Kurihara and Sekiguchi[21], Richardson and Whitman[26], and Vaid and Campanella[36] were plotted. The time dependency of the creep strength becomes larger in accordance with the plasticity index. The plasticity index depends on the properties of clay particles and absorbed water film around them, which is expressed by the difference in water content between the liquid limit and plastic limit. The clay particle with a large external activity attracts much moisture around it. The cohesive soils having this property indicate a large plasticity index. Bjerrum[5] pointed out that the creep rate of clay depends on the shear stress and thickness of the

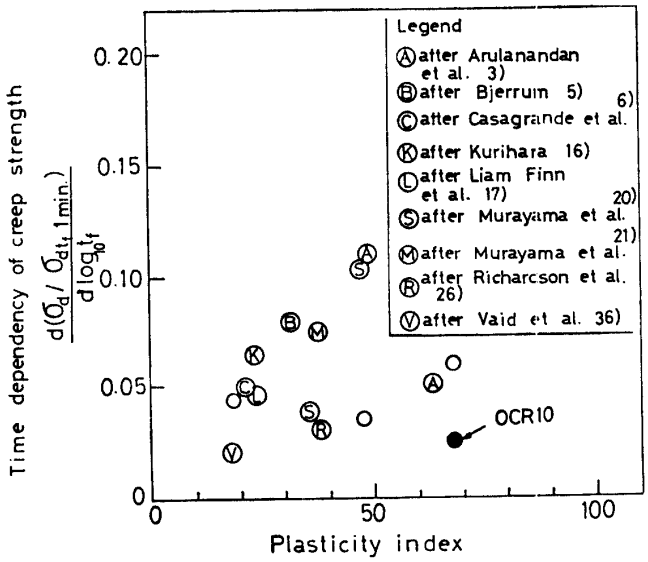

Fig. 23. Influence of plasticity index on time dependency of creep strength.

absorbed water film. Consequently, the time dependency of the creep strength has a relationship to the plasticity index of cohesive soils.

The time dependency of the creep strength for the over-consolidated Kirishima clay is smaller than that for the normally consolidated clay, because the viscosity component of the creep strength is to be changed by the stress history. Moreover, the time dependency of the creep strength depends on the consolidation pressure level as shown in Fig. 24. This figure was plotted by the result of the strain controlled triaxial compression test under the consolidation pressure of 1, 2, 3 and 8 kg/cm^2. The time dependency of the creep strength decreases exponentially to the consolidation pressure.

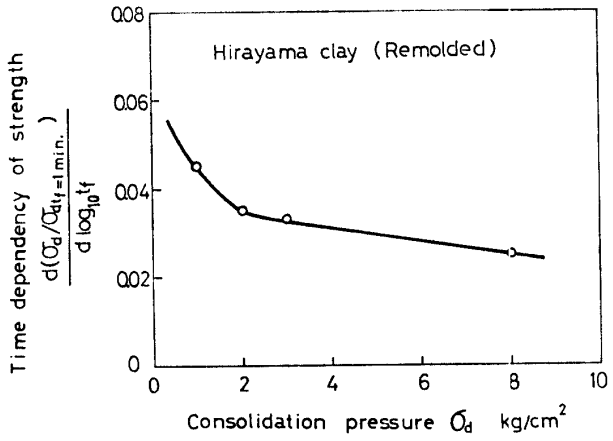

Fig. 24. Influence of consolidation pressure on time dependency of strength.

Part 3. Creep failure as a rate process

The purpose of this part is to derive the stress-strain-time relation for creep failure by means of a rate process theory. The formulas[7,18,20] derived by making use of this theory previously can not be applied to the creep failure, because the derivations of the formulas are based on the rheo-

logical models[7,20], and the force on each bond is constant in the process of creep deformation[7,18,20].

Therefore, in order to overcome these defects, the formulas are derived from the following standpoints:

(1) The rate process theory is valid for creep failure.

(2) Creep failure is fundamentally a non-linear phenomenon.

(3) The stress-strain-time relation for creep failure is not to be expressed by rheological models.

(4) The force acting on each bond is not constant in the process of creep failure.

The formulas derived are discussed in reference to the experimental results. Preliminary results of this part have been published before[28,29].

According to the rate process theory[18], the frequency of activation of a bond in the direction of stress is expressed by

$$\bar{\nu}=2\frac{kT}{h}exp\left(-\frac{\Delta F}{RT}\right)sinh\left(\frac{f\lambda}{2kT}\right) \tag{12}$$

where k is Boltzmann's constant, T the absolute temperature, h Planck's constant, ΔF the activation energy, R the gas constant, f the force acting on each bond and λ the average distance between bonds. If the force acting on each bond is large enough to cause creep deformation, the frequency of activation of a bond increases, and as a result the number of bonds per unit area decreases. Therefore,

$$sinh(f\lambda/2kT)=\frac{1}{2}exp(f\lambda/2kT) \tag{13}$$

As the frequency of activation of a bond at any time is equal to the ratio of the activated bonds for unit time to the total number of bonds per unit area, Eq. (12) becomes

$$\bar{\nu}=-\frac{1}{N}\frac{dN}{dt}=\frac{kT}{h}exp\left(-\frac{\Delta F}{RT}\right)exp\left(\frac{f\lambda}{2kT}\right) \tag{14}$$

where N is the number of bonds and t the time. Eq. (14) is the basic formula of the rate process theory.

In order to derive the stress-strain-time relation according to Eq. (14), some assumptions are necessary. Firstly, consider a model as shown schematically in Fig. 25, to connect the frequency of activation of a bond and strain. In Fig. 25, Eq. (14) expresses the frequency of activation due to the deformation on x_i plane. If the deformation progresses in the direction of the y-axis, the displacement for unit time due to the activation of a bond on x_i plane becomes λ'. If the number of bonds per unit length is s, the strain rate $\frac{d\varepsilon}{dt}$ is

$$\frac{d\varepsilon}{dt}=s\lambda'(\bar{\nu})=s\lambda'\left(-\frac{1}{N}\frac{dN}{dt}\right)=s\lambda'\frac{kT}{h}exp\left(-\frac{\Delta F}{RT}\right)exp\left(\frac{f\lambda}{2kT}\right) \tag{15}$$

if $s\lambda'=X$, Eq. (15)

$$\frac{d\varepsilon}{dt}=X(\bar{\nu})=X\left(-\frac{1}{N}\frac{dN}{dt}\right)=X\frac{kT}{h}exp\left(-\frac{\Delta F}{RT}\right)exp\left(\frac{f\lambda}{2kT}\right) \tag{16}$$

where ε is the strain. The parameter λ' is constant, and s and X decrease with the progress of deformation. Assume that

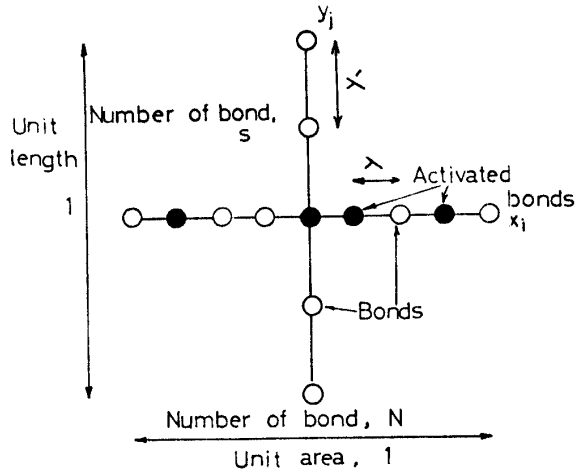

Fig. 25. Hypothetical picture of relationship between activation of bonds and strain.

$$X = b\frac{1}{t^m} \tag{17}$$

where b is the constant and m is the coefficient that decreases from 1 to 0.

It is considered that the force f acting on each bond differs with bonds. But, assuming that the force f is expressed by mean value, namely deviator stress σ_d divided by the number of bonds per unit area N in the triaxial compression state becomes

$$f = \frac{\sigma_d}{N} \tag{18}$$

Substituting Eq. (17) and Eq. (18) into Eq. (16) yields

$$\frac{d\varepsilon}{dt} = -b\frac{1}{t^m}\frac{1}{N}\frac{dN}{dt}$$

$$= b\frac{1}{t^m}\frac{kT}{h}\exp\left(-\frac{\Delta F}{RT}\right)\exp\left(\frac{\lambda}{2kT}\frac{\sigma_d}{N}\right) \tag{19}$$

From Eq. (16), the relationship between the strain and number of bonds per unit area is expressed by

$$N = N_0 e^{-\frac{\varepsilon t^m}{b}} \tag{20}$$

in which N_0 is the initial number of bonds per unit area. Substituting Eq. (20) into Eq. (19) yields

$$\frac{d\varepsilon}{dt} = b\frac{1}{t^m}\frac{kT}{h}\exp\left(-\frac{\Delta F}{RT}\right)\exp\left(\frac{\lambda}{2kT}\frac{e^{\frac{\varepsilon t^m}{b}}}{N_0}\sigma_d\right) \tag{21}$$

The resistance factor with respect to the external force is the number of bonds per unit area. According to Mitchell, Singh and Campanella[19], Ito and Matsui[13], the number of bonds per unit area N is in proportion to the effective consolidation pressure. Hence,

$$N_0 = a\sigma'_{m0} \tag{22}$$

where σ'_{m0} is the mean effective consolidation pressure and a the constant. Substituting Eq. (22) into Eq. (21)

$$\frac{d\varepsilon}{dt}=b\frac{1}{t^m}\frac{kT}{h}exp\left(-\frac{\Delta F}{RT}\right)exp\left(\frac{\lambda}{2kT}\frac{e^{\frac{\varepsilon t^m}{b}}}{a}\frac{\sigma_d}{\sigma'_{m0}}\right) \tag{23}$$

or

$$\frac{d\varepsilon}{dt}=b\frac{1}{t^m}\frac{kT}{h}exp\left(-\frac{\Delta F}{RT}\right)exp\left(\frac{\lambda}{2kT}\frac{e^{\frac{\varepsilon t^m}{b}}}{a}\frac{\sigma'_m}{\sigma'_{m0}}\frac{\sigma_d}{\sigma'_m}\right) \tag{24}$$

Transformation of Eq. (23) and Eq. (24) yields

$$\frac{d\varepsilon}{d\log t}=b\frac{1}{t^{m-1}}\frac{kT}{h}exp\left(-\frac{\Delta F}{RT}\right)exp\left(\frac{\lambda}{2kT}\frac{e^{\frac{\varepsilon t^m}{b}}}{a}\frac{\sigma_d}{\sigma'_{m0}}\right) \tag{25}$$

$$\frac{d\varepsilon}{d\log t}=b\frac{1}{t^{m-1}}\frac{kT}{h}exp\left(-\frac{\Delta F}{RT}\right)exp\left(\frac{\lambda}{2kT}\frac{e^{\frac{\varepsilon t^m}{b}}}{a}\frac{\sigma'_m}{\sigma'_{m0}}\frac{\sigma_d}{\sigma'_m}\right) \tag{26}$$

Taking logarithms of Eq. (23) and arranging it yields

$$\sigma_d=\frac{a\sigma'_{m0}}{\frac{\lambda}{2kT}e^{\frac{\varepsilon t^m}{b}}}\left(\log\frac{d\varepsilon}{dt}-\log b\frac{1}{t^m}\frac{kT}{h}exp\left(-\frac{\Delta F}{RT}\right)\right) \tag{27}$$

At failure, Eq. (25) becomes

$$\left(\frac{d\varepsilon}{d\log t}\right)_f=b\frac{1}{t_f^{m-1}}\frac{kT}{h}exp\left(-\frac{\Delta F}{RT}\right)exp\left(\frac{\lambda}{2kT}\frac{e^{\frac{\varepsilon_f t_f^m}{b}}}{a}\frac{\sigma_d}{\sigma'_{m0}}\right) \tag{28}$$

where t_f is the elapsed time to failure, ε_f the strain and $\left(\frac{d\varepsilon}{d\log t}\right)_f$ the logarithmic strain rate at failure. Taking logarithms of Eq. (28) and arranging it yields

$$\sigma_d=\frac{a\sigma'_{m0}}{\frac{\lambda}{2kT}e^{\frac{\varepsilon_f t_f^m}{b}}}\left(\log\left(\frac{d\varepsilon}{d\log t}\right)_f-(1-m)\log t_f-\log b\frac{kT}{h}exp\left(-\frac{\Delta F}{RT}\right)\right) \tag{29}$$

Eq. (29) gives the relationship between the creep strength and logarithmic elapsed time to failure, and explains the experimental results in Fig. 17, qualitatively. From Eq. (27) and Eq. (29)

$$\log t_f=-\frac{e^{\frac{\varepsilon_f t_f^m-\varepsilon t^m}{b}}}{1-m}\log\frac{d\varepsilon}{dt}+\frac{\log\left(\frac{d\varepsilon}{d\log t}\right)_f+\log b\frac{kT}{h}exp\left(-\frac{\Delta F}{RT}\right)\left(e^{\frac{\varepsilon_f t_f^m-\varepsilon t^m}{b}}-1\right)-m\,e^{\frac{\varepsilon_f t_f^m-\varepsilon t^m}{b}}\log t}{1-m} \tag{30}$$

is obtained. Eq. (30) explains theoretically the relationship between the elapsed time to creep failure and the steady state strain rate obtained experimentally by Saito and Uezawa[27]. This experimental result is shown in Fig. 26. According to Eq. (30), both m and $(\varepsilon_f t_f^m-\varepsilon t^m)$ decrease gradually to 0. Hence, the coefficient $\frac{e^{\frac{\varepsilon_f t_f^m-\varepsilon t^m}{b}}}{1-m}$ of the first term in the right hand of Eq. (30) approaches 1.

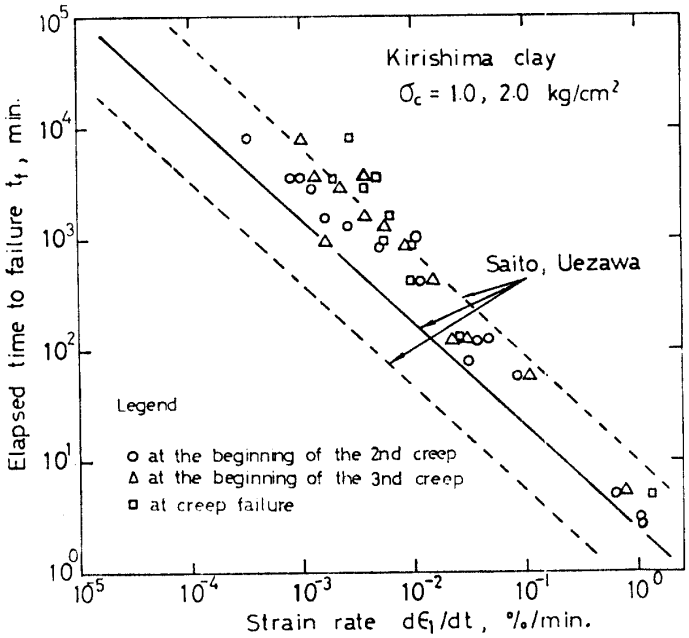

Fig. 26. Relationship between axial strain rate and elapsed time to creep failure for normally consolidated Kirishima clay.

Part 4. Relationship between the creep deformation of cohesive soils and landslide

In this part, the landslide displacement and time dependent strength are discussed in reference to the creep deformation and creep strength of cohesive soils.

1. Landslide displacement due to creep deformation

It is assumed that landslide displacement for a limited time is influenced by the landslide history, stress state, ground water level and landslide clays, etc. . In this case, the relationship between the landslide displacement and landslide clay is analyzed. In order to simplify this analysis, the landslide displacement after a large deformation, namely in the residual state is considered. The dilatancy deformation does not occur, or is small in this state. The creep strain is obtained as follows:

By substituting Eq. (10) into Eq. (11)

$$log_{10}\frac{d\gamma}{d\,log_{10}t}=\alpha+\frac{\sigma_d}{\frac{1}{\beta}} \tag{31}$$

Changing of Eq. (31) yields

$$\frac{d\gamma}{dt}=\frac{1}{2.3t}e^{2.3\left(\alpha+\frac{\sigma_d}{\frac{1}{\beta}}\right)} \tag{32}$$

By integrating Eq. (32)

$$\gamma-\gamma_b=e^{2.3\left(\alpha+\frac{\sigma_d}{\frac{1}{\beta}}\right)}(log_{10}t-log_{10}t_b) \tag{33}$$

where γ_b is the creep strain at a standard time t_b and α and $\frac{1}{\beta}$ the constants which depend on the

type of cohesive soils and stress history. The creep stress σ_d is constant. The relationship between the parameter $\frac{1}{\beta}$ and an apparent coefficient of viscosity is expressed by

$$\eta_{app.} = \frac{\sigma_d}{d\gamma/dt} = \frac{2.3t\sigma_d}{e^{2.3\left(\alpha+\frac{\sigma_d}{\frac{1}{\beta}}\right)}} \tag{34}$$

According to Eq. (34), the larger is the parameter $\frac{1}{\beta}$, the larger is the apparent coefficient of viscosity, if the other conditions are the same. Now, the parameter $\frac{1}{\beta}$ decreases exponentially in accordance with the plasticity index in Fig. 13. Consequently, the larger is the parameter α, creep stress σ_d and plasticity index, and the smaller is the parameter $\frac{1}{\beta}$ and apparent coefficient of viscosity, the larger is the creep strain $(\gamma-\gamma_b)$ for a limited time. Fig. 27 shows the relationship between the apparent coefficient of viscosity of landslide clays and an annual landslide displacement in Japan after Takenouchi[35]. The annual landslide displacement is inversely as the apparent coefficient of viscosity on a log-log scale. As the apparent coefficient of viscosity is closely related to the parameter $\frac{1}{\beta}$ and plasticity index of cohesive soils, the annual displacement becomes larger in accordance with the plasticity index of cohesive soils.

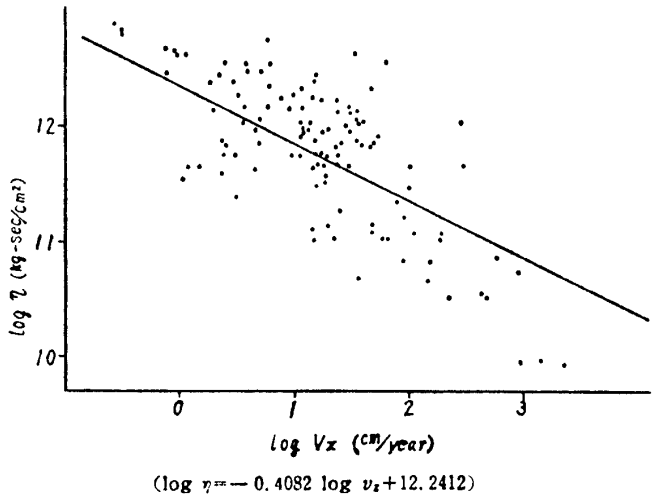

Fig. 27. Relationship between viscosity η and an annual displacement V_z of landslides (after Takenouchi[35]).

Fig. 28 shows the positions of landslide clays on the plasticity chart. The examples cited here are the Matsunoyama landslide[15], Sarukuyoji landslide[23] and Oami landslide[10] consisting of Tertiary sedimentary stratum, the Soryo landslide[12] and Gongenyama landslide[14] consisting of volcanic clastic materials, the Myoban landslide[25] consisting of volcanic clastic materials (thermal spring), and the landslides[24,40] in Tokushima-ken, Kochi-ken and the Obuchi landslide consisting of Paleozoic sedimentary stratum (fracture zone). The plasticity index of landslide clays differs according to the geological formations. In other words, the clays of the Tertiary type landslides are high plastic soils with a plasticity index of over 25. Contrary to them, the clays of the fracture zone type landslides are medium and low plastic soils with the plasticity index of under 15 per cent. The plasticity index of landslide clays consisting of volcanic clastic materials lie in the region between the clays of the Tertiary type landslide and those of the fracture zone type landslide.

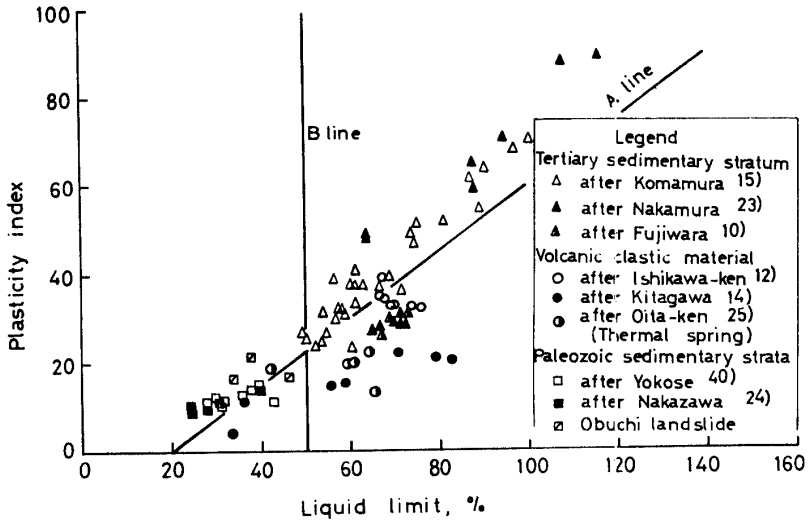

Fig. 28. Plasticity chart of landslide clays.

Therefore, the landslide displacement for a limited time becomes smaller in the following order, the Tertiary type landslides, landslides consisting of volcanic clastic materials and the fracture zone type landslides.

2. Time dependent strength for slope stability analysis

The shearing strength of landslide clay must be obtained for an analysis of slope stability. The shearing strength of soil is divided into that of the virgin specimen and residual strength by the existence of stress history. Skempton[34] pointed out the importance of residual strength to slope stability analysis. There are methods by means of the direct shear test[34], ring shear test[4] and triaxial shear test[8,9,39] for measurement of the residual strength. A standard for the selection of the shearing strength for slope stability analysis depends on the stress and deformation states, etc.. The evaluation of slope stability by the residual strength gives the safest value.

In order to improve slope stability analysis, the time dependent strength of landslide clays must be considered. The shearing strength parameters are the effective cohesion intercept c' and angle of effective shearing resistance ϕ'. The failure criterion of Mohr-Coulomb is expressed by

$$\frac{1}{2}\sigma_{df}=\frac{c'\cos\phi'-\sigma_3'\sin\phi'}{1-\sin\phi'} \tag{35}$$

where σ_3' is the effective minimum principal stress and σ_{df} expresses the creep strength. Now, neglecting the effective cohesion intercept c' yields

$$\sin\phi'=\frac{\sigma_1'-\sigma_3'}{\sigma_1'+\sigma_3'} \tag{36}$$

where σ_1' is the effective maximum principal stress. Reforming Eq. (36)

$$\sin\phi'=\frac{\sigma_{df}/\sigma_m'}{6+\sigma_{df}/\sigma_m'},\quad \sigma_{df}=\sigma_1'-\sigma_3' \tag{37}$$

As the effective stress ratio σ_{df}/σ_m' at failure is constant, the angle of effective shearing resistance is time independent. By reforming Eq. (35)

$$c' = \frac{\sigma_{df}\left(1-\frac{2}{3}\sin\phi'\right)-\sigma'_m \sin\phi'}{2\cos\phi'} \tag{38}$$

is obtained. The effective cohesion intercept c' is time dependent, because the creep strength σ_{df} and effective mean principal stress σ'_m are time dependent. Casagrande and Wilson[6] pointed out that the shear strength of cohesive soils reduces to 40~80 per cent of its normal value. Now, if $\phi'=15°$, $\sigma_{df}/\sigma'_m=2.1$ and σ_{df} decreases from the normal value of 2.1 kg/cm^2 to 1.47 kg/cm^2 of its 70 per cent, the effective cohesion intercept decreases from the normal value of 0.765 kg/cm^2 to 0.536 kg/cm^2 (about 70 per cent of normal value). According to Fig. 23, the time dependency of the creep strength becomes larger in accordance with the plasticity index of cohesive soils. Therefore, the larger is the plasticity index of cohesive soils, the larger becomes the time dependency of the effective cohesion intercept.

Summary

This paper is related to the creep deformation and creep strength of cohesive soils and their relationship to landslide. In order to accomplish these subjects, the experimental and theoretical studies by the rate process theory were carried out. The results are summarized as follows:

1) The creep deformation of cohesive soils are to be grouped into the following four types according to the pattern of the creep strain-logarithmic time relation; (i) it is linear without the creep stress level, (ii) it is linear under the low creep stress levels, but it changes showing such as the singmoid curve under the high creep stress levels, (iii) the strain occurs momentarily and (iv) it is linear in the preloaded and residual states that the dilatancy deformation does not occur.

2) The creep deformation is to be influenced by the five components of elasticity, retarded elasticity (time dependent), time independent dilatancy, time dependent dilatancy and viscosity. The properties and degree of mobilization of their components depend on the soil properties and stress states, etc..

3) The logarithmic excess pore water pressure rate increases with creep stress in the first creep region, but it is constant without creep stress in the second creep region. Consequently, the creep strain-logarithmic time relation exhibits linearity under the low creep stress levels and non-linearity under the high creep stress levels. In the second creep region, it is linear without creep stress. The logarithmic creep rate in the second creep region is influenced by the retarded elasticity, time dependent dilatancy and viscosity.

4) The creep stress dependency of the logarithmic creep rate in the second creep region depends on the plasticity index of the cohesive soils and stress state, etc.. The parameter $\frac{1}{\beta}$ is in a similar parameter as the apparent coefficient of viscosity is.

5) The mobilization process of internal friction (effective stress ratio σ_d/σ'_m) for normally consolidated clay differs from that for the over-consolidated clay.

6) The effective stress ratio at the beginning of the second and third creep regions and creep failure are constant without the creep stress level, respectively, but the creep strains at these critical points depend on the creep stress.

7) The creep strength of cohesive soil is composed of the friction, dilatancy and viscosity components. Their friction and dilatancy components are time independent. Hence, the time dependency of the creep strength is only influenced by the viscosity component. And, the larger

is the plasticity index of the cohesive soils, the larger is the time dependency of the creep strength.

8) The stress-strain-time relationship for creep failure was derived by applying the rate process theory. This formula gives a theoretical background to the experimental results of the creep failure.

9) The displacement of the creep type landslide is influenced by the creep stress dependency of the logarithmic strain rate and by the plasticity index of the landslide clays.

10) The effective cohesion intercept of the shearing strength parameters is time dependent.

Acknowledgements

The author wishes to express his appreciation to Professor K. Sue, Kyushu University and Professor M. Haruyama, Kagoshima University for their kind guidance and encouragement during this investigation. The author also wishes to thank Professor T. Fujikawa and Associate Professor M. Takayama, Kyushu University for their advice and helpful suggestions. The author further wishes to express his gratitude to Emeritus Professor S. Murayama, Kyoto University and Professor H. Fujimoto, Miyazaki University for their kind guidance. The author is indebted to Associate Professer K. Takeshita, Kyushu University, K. Uehara and S. Maeda, Nagasaki Prefectural Office for samplings of landslide clays.

References

1) Akai, K., Adachi, T. and Ando, N.: A stress-strain-time relation of saturated clays (in Japanese). *Trans. Japan Soc. Civil Eng.*, **225**, 53–61 (1974)
2) Akai, K., Adachi, T., Tanaka, T. and Ikeda, G.: Time dependent behavior of over-consolidated clay (in Japanese). *Proc. 10th Conf. Japan Soc. Soil Mech. Found. Eng.*, 241–244 (1975)
3) Arulanandan, K., Shen, C. K. and Young, R. B.: Undrained creep behaviour of a coastal organic silty clay. *Geotechnique*, **21(4)**, 359–375 (1971)
4) Bishop, A. W., Green, G. E., Garga, V. K., Andresen, A. and Brown, J. D.: A new ring shear apparatus and its application to the measurement of residual strength. *Geotechnique*, **21(4)**, 273–328 (1971)
5) Bjerrum, L.: General reports. *Proc. 8th Int. Conf. Soil Mech. Found. Eng.*, **vol. 3,** 111–159 (1973)
6) Casagrande, A. and Wilson, S. D.: Effect of rate of loading on the strength of clays and shales at constant water content. *Geotechnique*, **2(3)**, 251–263 (1951)
7) Christensen, R. W. and Wu, T. H.: Analysis of clay deformation as a rate process. *Jour. Soil Mech. Found. Div., A.S.C.E.*, **90(SM6)**, 125–157 (1964)
8) Fujikawa, T. and Gibo, S.: On the determination of residual strength by stress analysis of failure surface (in Japanese). *Trans. Japan Soc. Irri. Drain. Recla. Eng.*, **57**, 33–38 (1975)
9) Fujikawa, T. and Gibo, S.: On the determination of residual strength by triaxial compression test (in Japanese). *Trans. Japan Soc. Irri. Drain. Recla. Eng.*, **57**, 39–45 (1975)
10) Fujiwara, A.: Investigations of landslides and their analyses (in Japanese). p. 163–179, Richotosho, Tokyo (1970)
11) Goldstein, M. and Ter-Stepanian, G.: The long-term strength of clays and depth creep of slopes. *Proc. 4th Int. Conf. Soil Mech. Found. Eng.*, **vol. 2,** 311–314 (1957)
12) Ishikawa-ken: Soryo landslide (in Japanese). p. 1–92, Ishikawa-ken, (1970)
13) Ito, T. and Matsui, T.: Plastic flow mechanism of clays (in Japanese). *Trans. Japan Soc. Civil Eng.*, **236**, 109–123 (1975)
14) Kitagawa, K.: Relation between geology and ground water in Gongenyama landslide (in Japanese). *Proc. 5th Conf. Japan Soc. Chisan*, 89–97 (1966)
15) Komamura, F.: On characteristics of Matsunoyama landslide clay (in Japanese). *Jour. Japan Soc. Landslide*, **3**, 8–20 (1965)

16) Kurihara, N.: Experimental study on creep rupture of clays (in Japanese). *Trans. Japan Soc. Civil Eng.*, **202**, 59–71 (1972)
17) Liam Finn, W. D. and Shead, D.: Creep and creep rupture of an undisturbed sensitive clay. *Proc. 8th Int. Conf. Soil Mech. Found. Eng.*, **vol. 2**, 135–142 (1973)
18) Mitchell, J. K., Campanella, R. G. and Singh, A.: Soil creep as a rate process. *Jour. Soil Mech. Found. Div., A.S.C.E.*, **94(SM1)**, 231–253 (1968)
19) Mitchell, J. K., Singh, A. and Campanella, R. G.: Bonding, effective stresses, and strength of soils. *Jour. Soil Mech. Found. Div., A.S.C.E.*, **95(SM5)**, 1219–1246 (1969)
20) Murayama, S. and Shibata, T.: On the rheological characters of clay (in Japanese). *Trans. Japan Soc. Civil Eng.*, **40**, 1–31 (1956)
21) Murayama, S., Kurihara, N. and Sekiguchi, H.: On creep rupture of normally consolidated clays (in Japanese). *Bull. Disaster Prevent. Research Inst. Kyoto Univ.*, **13B**, 525–541 (1970)
22) Murayama, S., Sekiguchi, H. and Ueda, T.: A study of the stress-strain-time behavior of saturated clays based on a theory of nonlinear viscoelasticity. *Jour. Japan Soc. Soil Mech. Found. Eng.*, **14(2)**, 19–33 (1974)
23) Nakamura, H.: Geotechnical properties of the landslides, especially Sarukuyoji landslide, observed in the areas composed of black mudstone (in Japanese). *Jour. Japan Soc. Landslide*, **30**, 33–43 (1972)
24) Nakazawa, T.: On general properties of landslides in the central part, Shikoku (in Japanese). *Proc. 6th Conf. Japan Soc. Chisan*, 182–185 (1967)
25) Oita-ken: On Myoban landslide (in Japanese). p. 1–124, Oita-ken, (1967)
26) Richardson, A. M. and Whitman, R. V.: Effect of strain-rate upon undrained shear resistance of a saturated remolded fat clay. *Geotechnique*, **13**, 310–324 (1961)
27) Saito, M. and Uezawa, H.: Failure of soil due to creep. *Proc. 5th Int. Conf. Soil Mech. Found. Eng.*, **vol. 1**, 315–318 (1961)
28) Shimokawa, E.: On the rheological properties of soil and their relation to slope failure (in Japanese). *Jour. Japan Soc. Erosion Control*, **84**, 6–13 (1972)
29) Shimokawa, E.: Creep failure of soil (in Japanese). *Proc. 27th Conf. Japan Soc. Civil Eng.*, **vol. 3**, 141–144 (1972)
30) Shimokawa, E.: Creep failure of saturated clays from an effective stress point of view (in Japanese). *Bull. Fac. Agr. Kagoshima Univ.*, **29**, 199–216 (1979)
31) Shimokawa, E.: Creep deformation of soils (in Japanese). *Bull. Experimental Forests Kagoshima Univ.*, **7**, 1–28 (1979)
32) Singh, A. and Mitchell, J. K.: General stress-strain-time function for soils. *Jour. Soil Mech. Found. Div., A.S.C.E.*, **94(SM1)**, 21–46 (1968)
33) Singh, A. and Mitchell, J. K.: Creep potential and creep rupture of soils. *Proc. 7th Int. Conf. Soil Mech. Found. Eng.*, **vol. 1**, 379–384 (1969)
34) Skempton, A. W.: Long term stability of clay slopes. *Geotechnique*, **14**, 77–101 (1964)
35) Takenouchi, T.: On viscosity coefficients of clays of landslide area in Japan (in Japanese). *Jour. Japan Soc. Landslide*, **7**, 31–36 (1966)
36) Vaid, Y. P. and Campanella, R. G.: Time-dependent behaviour of undisturbed clay. *Jour. Geotech. Eng. Div., A.S.C.E.*, **103(GT7)**, 693–709 (1977)
37) Vyalov, S. S., Pekarskaya, N. K. and Maximyak, R. V.: On the failure process in clayey soils. *Proc. 4th Asian Regional Conf. Soil Mech. Found. Eng.*, **vol. 1**, 95–97 (1971)
38) Walker, L. K.: Secondary compression in the shear of clays. *Jour. Soil Mech. Found. Div., A.S.C.E.*, **95(SM1)**, 167–188 (1969)
39) Webb, D. L.: Residual strength in conventional triaxial tests. *Proc. 7th Int. Conf. Soil Mech. Found. Eng.*, **vol. 1**, 433–441 (1969)
40) Yokose, H.: On characteristics of soils in landslide area (in Japanese). *Jour. Japan Soc. Soil Mech. Found. Eng.*, **54**, 3–9 (1962)
41) Young, R. N. and Warkentin, B. P.: Introduction to soil behavior. p. 328, The Macmillan Company, New York (1966)